2009 American Control Conference
Hyatt Regency Riverfront, St. Louis, MO, USA
June 10-12, 2009

Sensor Maneuver Design for Microwave Source Localization

N. Eva Wu, Jong-Yeob Shin, and Kun Huang

Abstract— **This paper presents a solution to maneuvering networked airborne sensors with both time and motion constraints to benefit sensing. Decentralized maneuver design is shown to enhance the network tolerance to loss of sensors, in addition to reducing the complexity in computation and communications. Sensing accuracy and speed are achieved by a high-level aggregation of the sensor outputs and a time-coordinated bang-bang control of the sensor carrying vehicles to their best sensing states. The solution is demonstrated through a network of airborne location sensors, where the sensors are paired to acquire time difference of arrival and frequency difference of arrival of microwave signals for localization of their emitters to a required accuracy in minimum time. Network resilience to localizing emitters in the face of vehicle loss is shown via simulations of a six-sensor network with respect to a range of vehicle loss probabilities.**

Keywords: tolerance to sensor loss, source localization, maneuver design, airborne sensors, decentralization

I. INTRODUCTION

Passive localization of microwave emitters is a mature technology [11]. With networks of unmanned aerial vehicles (UAVs) replacing stationary sensor networks and manned vehicles, however, significant improvements can be expected in both speed and accuracy of sensing through tasking, guidance, and control of the cooperative sensors. Networking in a hostile environment, however, poses additional challenges. Data exchange inherent to a networked operation and prolonged mission time due to poor data quality expose the otherwise passive location sensors, thus increase the likelihood of the vehicles being destroyed.

Fault-tolerant tasking and guidance of networked airborne location sensors have been considered by the first author and coworkers recently [17], where sensors are paired to localize microwave emitters by intercepting and processing time difference of arrival and frequency difference of arrival of their signals. Two measures have been taken there to enhance the network availability in the face of loss of sensors which effectively changes the network architecture and thus degrades the sensing performance. The first measure amounts to solving a Markov decision problem [2] that allocates sensors to randomly emerging emitters to minimize the effect of sensor loss. The second measure is taken based on that sensor states (positions, velocities) at which emitter signals are acquired can have significant effect on the data quality [16], and that sensors allocated to a target must continue to adjust their trajectories until the target is deemed localized by a stopping criterion. A weighted sum of volumes of concentration ellipsoids [13] formed by the predicted localization errors is used in [17] as a guidance criterion for maneuvering the vehicles, where the weights draw on the knowledge of vehicle loss probability.

This paper tackles two issues that remain unresolved in the aforementioned work. First, the complexity of the algorithm in [17] for generating sensor trajectories prohibits its real-time exercise as the number of participating sensors increases, undermining the benefits afforded by the large number of mobile sensors. Moreover, vehicle maneuver schemes are yet to be developed to steer the sensors along their desired trajectories in a time coordinated manner.

The complexity issue encountered in [17] is resolved in this paper by decentralization: emitter location estimation and sensor trajectory generation are both carried out between individual pairs of sensors independently, disregarding the presence of the rest of the sensors. An aggregation scheme with significantly reduced data exchange [4] is then applied to best recover the location accuracy afforded by a centralized scheme. The term *decentralized sensing* is to be used throughout the paper with the understanding that it implies decentralization in sensing, processing, as well as sensor trajectory generation. It is the decentralized sensor trajectory generation that offers the most significant reduction in complexity and enhancement in fault-tolerance.

The vehicle control issue is resolved in this paper under a far-field and small-update-interval condition [9] that upholds the dominance of sensor velocities over sensor positions in affecting the accuracy of emitter localization. Under this condition, convex velocity reachable sets can be efficiently computed, based on which a 4-variable sensor state optimization can be solved between two paired sensors. Vehicle control using the bang-bang strategy can be implemented for all vehicles to arrive simultaneously at their respective destination velocities, which mark the onset of a new round of target signal acquisition. Time-coordination is necessary for localizing non-stationary emitters, in addition to minimizing operation delays. Time-coordination is also recognized as an important design constraint in a number of other applications involving the control of unmanned aerial vehicles [1].

This paper is organized as follows. Section II reviews the centralized emitter localization problem. This part of the presentation draws heavily from [17] to explain the background, describe the problem, and highlight the challenges that have not been addressed previously. Section III delineates the

Manuscript received March 12, 2009

N. Eva Wu and Kun Huang are with the Department of Electrical and Computer Engineering, Binghamton University, SUNY, Binghamton, NY 13902, USA, evawu,khuang2@binghamton.edu, and Jong-Jeob Shin is with Gulfstream Aerospace Coperation, jong.yeob.shin@gulfstream.com

new decentralized solution to emitter localization, including aspects of aggregation of estimates, assessment of location accuracy, generation of sensor trajectories, control of vehicles to reach the projected sensor states, and finally a numerical example through a 6-sensor network to verify the network fault-tolerance. Section IV concludes the paper by analyzing the benefit and the cost of the decentralized solution.

II. Problem Description

Much of the material in the first two subsections in this section is drawn from [17]. Overall, the purpose of this section is to help explain the background, formulate a basic maneuver design problem, and state new development to be made in the subsequence sections.

A. Measurement models

Figure 1 depicts an emitter localization mission in a simplified setting, where the motion of two vehicles and an emitter lie within a plane. If the two vehicles are equipped to acquire both the time difference of arrival (TDOA) and the frequency difference of arrival (FDOA) of the emitter's signal based on the following error-free signal models, the emitter can be immediately localized.

$$s_T = \frac{1}{c}[\sqrt{(x_2-x_e)^2+(y_2-y_e)^2}-\sqrt{(x_1-x_e)^2+(y_1-y_e)^2}], \tag{1}$$

and

$$s_F = \frac{f_e}{c}[\frac{(x_2-x_e)u_2+(y_2-y_e)v_2}{\sqrt{(x_2-x_e)^2+(y_2-y_e)^2}}-\frac{(x_1-x_e)u_1+(y_1-y_e)v_1}{\sqrt{(x_1-x_e)^2+(y_1-y_e)^2}}], \tag{2}$$

where (x_e,y_e) is the emitter location to be estimated, (x_1,y_1) and (x_2,y_2) are the positions of the two vehicles, respectively, (u_1,v_1) and (u_2,v_2) are the velocities of the vehicles, f_e is the carrier frequency of the emitted signal, and c is the speed of light. The sensors mounted on the vehicles are passive nodes when acquiring data from the target, but become active when exchanging data between them in order to provide a location estimate.

Typically several thousand signal samples acquired in a fraction of a second by the two sensors are cross-correlated to obtain the maximum likelihood estimates of time difference of arrival and frequency difference of arrival [14]. With a large number of signal samples, the estimates on the time difference of arrival and frequency difference of arrival can assume to have a Gaussian additive error whose covariance achieves the Cramer-Rao lower bound [10].

Consider a set of $2N$ measurements collected by a network of N pairs of sensors in the presence of additive errors

$$\mathbf{r} = \mathbf{g}(\mathbf{p}_e;\mathbf{z})+\mathbf{n} = \begin{bmatrix} s_T^1(\mathbf{p}_e;\mathbf{z}_1,\mathbf{z}_2) \\ s_F^1(\mathbf{p}_e;\mathbf{z}_1,\mathbf{z}_2) \\ \vdots \\ s_T^N(\mathbf{p}_e;\mathbf{z}_{2N-1},\mathbf{z}_{2N}) \\ s_F^N(\mathbf{p}_e;\mathbf{z}_{2N-1},\mathbf{z}_{2N}) \end{bmatrix} + \begin{bmatrix} n_T^1 \\ n_F^1 \\ \vdots \\ n_T^N \\ n_F^N \end{bmatrix}, \tag{3}$$

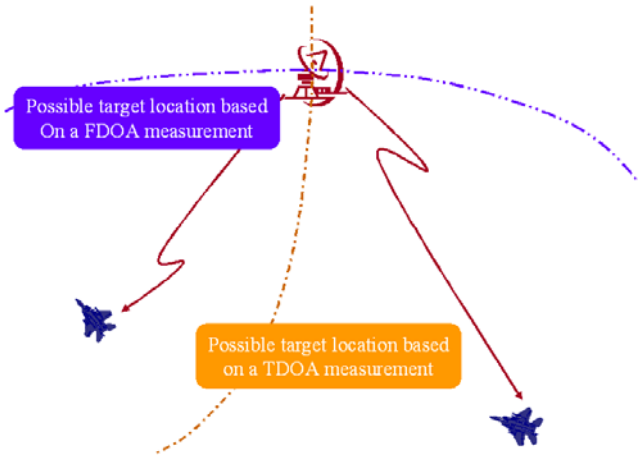

Fig. 1. Emitter location based on a TDOA measurement and an FDOA measurement by two sensors.

where $\mathbf{p}_e=(x_e,y_e)$ is the emitter location, $\mathbf{z}_i \equiv (x_i,y_i,u_i,v_i)$ is the state of the ith sensor, s_T^i and s_F^i are the time and frequency measurement models defined in (1) and (2), respectively. $\mathbf{z}=(\mathbf{z}_1,\mathbf{z}_2,\cdots,\mathbf{z}_{2N})$ denotes the Cartesian product.

In case the estimate of emitter location based on one batch of signal samples does not meet the accuracy requirement, sensors must be given time to adjust their states to be effective in acquiring new information that helps improve the accuracy, or must abort the mission if a time limit has been reached. Assume that a stopping criterion has been set for this purpose.

Based on initial estimate $\hat{\mathbf{p}}_e$, and measurement error covariance C, which can be evaluated from signal samples [8], an emitter localization problem can be cast as an extended Kalman filtering problem [1] that updates the current estimate at time t to $\hat{\mathbf{p}}_e^+$ at time t^+ based on the following state and measurement models,

$$\mathbf{p}_e^+ = \mathbf{p}_e+w,\ \ w\sim N(0,Q), \tag{4}$$
$$\mathbf{r} = \mathbf{g}(\mathbf{p}_e;\mathbf{z})+\mathbf{n},\ \ \mathbf{n}\sim N(0,C) \tag{5}$$

in the case of a stationary target, which lead to the following estimator, where Q is a design parameter for adjusting the

[1]The use of recursive formulation of the estimation problem is a departure from [17]. (Extended) Kalman filters have been widely applied in many fields, including mapping algorithms used in synthetic aperture radar (SAR) [7] and simultaneous localization and mapping (SLAM) [6], where uncertainties in sensor states present a significant technical challenge. Sensor state uncertainties have also been discussed in the localization problem of microwave emitter [16]. This paper, however, applies extended Kalman filtering algorithms to serve two different purposes alternately: to estimate emitter location with the exact knowledge of the sensor states, and to calculate the next sensor state with the approximate knowledge of the emitter location. The main interest of the paper is in the latter, which will be discussed in greater detail.

convergence property [18].

$$\hat{\mathbf{p}}_e^+ = \hat{\mathbf{p}}_e + K[\mathbf{r}^+ - \mathbf{g}(\hat{\mathbf{p}}_e;\mathbf{z})], \quad (6)$$

$$P^+ = [P^{-1} + G^T(\hat{\mathbf{p}}_e;\mathbf{z})C^{-1}G(\hat{\mathbf{p}}_e;\mathbf{z})]^{-1}, \quad (7)$$

$$K = [P+Q]G^T[G(P+Q)G^T + C]^{-1}, \quad (8)$$

where

$$G(\hat{\mathbf{p}}_e;\mathbf{z}) \equiv \frac{\partial \mathbf{g}(\mathbf{p}_e;\mathbf{z})}{\partial \mathbf{p}_e}\,|_{\mathbf{p}=\hat{\mathbf{p}}_e}\,. \quad (9)$$

The velocity of a moving target of a constant velocity can be calculated from target positions evaluated at two consecutive acquisition cycles assuming that product of the target speed and each acquisition duration is well within the tolerable localization error.

B. Criterion for sensor maneuver

For a given $\kappa > 0$,

$$R_\kappa \equiv \{\mathbf{p} | [\mathbf{p} - E(\mathbf{p})]^T P^{-1} [\mathbf{p} - E(\mathbf{p})] \le \kappa\} \quad (10)$$

defines an ellipsoid with semi-axis $\sqrt{\kappa\lambda_i}$, where λ_i is the ith largest eigenvalue of P. R_κ is called a concentration error ellipsoid, and is often used to indicate the accuracy of an estimate for a specified value of probability [13] when P is regarded as the covariance of a Gaussian distribution associated with unbiased estimate. In the two-dimensional setting of Fig.1, for example, $area(R_\kappa) = \pi\kappa\sqrt{det(P)}$, and $Pr[\mathbf{p} \in R_{\ln 4}] = 0.5$.

Denote by $\mathscr{A}_i(\tau)$ for sensor i the set of states reachable by the airborne sensor within a specified amount of time τ from its current state $\mathbf{z}_i$ under some speed and curvature constraints.

Assuming $\mathscr{A}_i(\tau)$ available, a criterion is sought in [17] under which the states $\mathbf{z}_i$, $i = 1, \cdots, 2N$ of all sensors allocated to a detected emitter are to be adjusted within τ seconds to $\mathbf{z}_i^+ \in \mathscr{A}_i(\tau)$ to best improve emitter location estimate, referenced at the current location estimate. Since $\sqrt{det(P)}$ is proportional to the volume of the ellipsoid R_κ defined by P [3], define projected covariance

$$P(\hat{\mathbf{p}}_e, \mathbf{z}^+) \equiv [P^{-1}(\hat{\mathbf{p}}_e, \mathbf{z}) + G^T(\hat{\mathbf{p}}_e;\mathbf{z}^+)C^{-1}G(\hat{\mathbf{p}}_e;\mathbf{z}^+)]^{-1}, \quad (11)$$

at t^+, from which $\mathbf{z}^+$ is calculated by

$$\min_{\mathbf{z}_i^+ \in A_i,\, \forall i} V(\hat{\mathbf{p}}_e, \mathbf{z}^+) = \min_{\mathbf{z}_i^+ \in A_i,\, \forall i} \sqrt{\det P(\hat{\mathbf{p}}_e, \mathbf{z}^+)}. \quad (12)$$

V is used to denote the objective function for optimizing the sensor state at the most recent location estimate. The sensors are then thrust to the projected states, from which new target data are acquired to update location estimate to $\hat{\mathbf{p}}_e^+$ based on (6)–(8).

Suppose during the course of reaching $\mathbf{z}^+$, the probability of loss of any sensor pair is p, and this probability remains the same in subsequent intervals of sensor state update. For a given number m of remaining sensor pairs in the network, $m = 1, \cdots, N$, a distinct expression of guidance criterion can be written for each of the $2^m - 1$ viable outcomes of Bernoulli trials. Let the probability mass function be p_i for the ith viable outcome, $i = 0, \cdots, 2^m - 1$.

Further, denote by $\Pi_i \mathbf{z}$ the projection of the stacked up sensor state resulting from the ith viable outcome upon loss of a specific set of sensor pairs. A weighted sum of all possible viable outcomes by their respective likelihood of occurrences is established as a fault-tolerant guidance criterion.

$$\min_{\mathbf{z}_i^+,\, \forall i} L(\hat{\mathbf{p}}_e, \mathbf{z}^+),\ L(\hat{\mathbf{p}}_e, \mathbf{z}^+) = \sum_{i=0}^{2^{m-1}} V(\hat{\mathbf{p}}_e, \Pi_i \mathbf{z}^+) p_i. \quad (13)$$

Each volume is associated with a network of a specific configuration.

C. Difficulties in solving for $\mathbf{z}^+$

Both the computation and the representation of reachable set $\mathscr{A}_i(\tau)$ that forms the explicit domain for optimizing the projected state at t^+ are too processing and memory intensive to implement in real time. In addition, objective function (13) is seen to be highly complex and non-convex with respect to $\mathbf{z}^+$, even in its unweighted form (12).

Furthermore, from expressions (6)–(8) for location estimation, and expressions (11)–(12) for projected sensor state calculation, processing demand is seen to grow with the size of the network, and the need for significant data exchange among sensors can result in severe time delays and exposure of the sensors to adversaries.

Decentralization of network operation is proposed to overcome the above difficulties, which grants autonomous to each pair of sensors; furthermore, sensor positions are abandoned and only sensor velocities are retained as the optimization variables in solving (13). Together they reduce the number of optimization variables from $8N$ to 4, and limit the need for data exchange to mostly between the two sensors in a pair.

The abandonment of sensor positions must be conditioned on the dominance of sensor velocities over sensor positions, which requires that all vehicles are sufficiently far from both the emitter location and its estimate, and that the update interval of a vehicle state is sufficiently small, resulting in a small position change relative to the range with respect to the emitter. These will be referred to as the *far-field small-update-interval* condition.

Fig.2 helps clarify the rather complicated localization process by showing the sequence of events and typical inter-event times. This timing diagram will be revisited in the next section.

III. Achieving fault-tolerance through decentralization

This section presents a complete solution to decentralized localization under the far-field small-update-interval condition. The presentation follows the order of the occurrence of the event sequence depicted in the timing diagram in Fig.2.

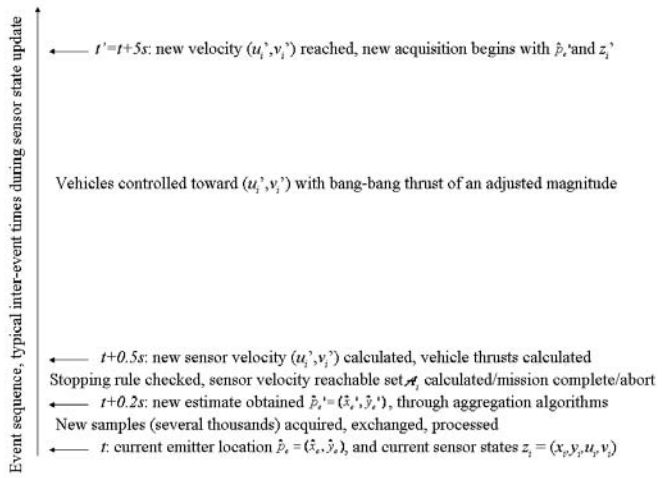

Fig. 2. Sequence of events and approximate time span of each event within a sensor state update period.

A. Decentralized location estimation

Suppose the first event in Fig.2 has occurred: an initial estimate or initial guess of the location of an emitter is obtained, along with an initial error covariance, initial states of the participating pre-paired sensors. This subsection describes how the first event leads to the second event upon which a newly aggregated estimate of emitter location is obtained with an aggregated error covariance. Let

$$\mathbf{g}^j(\mathbf{p}_e;\mathbf{z}_{2j-1},\mathbf{z}_{2j}) = (s_T^j(\mathbf{p}_e;\mathbf{z}_{2j-1},\mathbf{z}_{2j}), s_F^j(\mathbf{p}_e;\mathbf{z}_{2j-1},\mathbf{z}_{2j})),$$

and

$$\mathbf{n}^j = (n_T^j, n_F^j), \quad C^j = E[(\mathbf{n}^j)(\mathbf{n}^j)^T].$$

Rewriting the measurement model of the jth sensor pair

$$\mathbf{r}^j = \mathbf{g}^j(\mathbf{p}_e;\mathbf{z}_{2j-1},\mathbf{z}_{2j}) + \mathbf{n}^j, \ \mathbf{n}^j \sim N(0, C^j), \tag{14}$$

for which a decentralized estimator is

$$\begin{aligned}
&(\hat{\mathbf{p}}_e^j)^+ = \hat{\mathbf{p}}_e + K^j[(\mathbf{r}^j)^+ - \mathbf{g}^j(\hat{\mathbf{p}}_e;\mathbf{z}_{2j-1},\mathbf{z}_{2j})] \\
&(P^j)^+ = [P^{-1} + G^j(\hat{\mathbf{p}}_e;\mathbf{z}_{2j-1},\mathbf{z}_{2j})^T (C^j)^{-1} G^j(\hat{\mathbf{p}}_e;\mathbf{z}_{2j-1},\mathbf{z}_{2j})]^{-1} \\
&K^j = [P+Q](G^j)^T[(G^j)(P+Q)(G^j)^T + C^j]^{-1}
\end{aligned} \tag{15}$$

where

$$G^j(\hat{\mathbf{p}}_e;\mathbf{z}_{2j-1},\mathbf{z}_{2j}) \equiv \frac{\partial \mathbf{g}^j(\mathbf{p}_e;\mathbf{z}_{2j-1},\mathbf{z}_{2j})}{\partial \mathbf{p}_e}\,|_{\mathbf{p}=\hat{\mathbf{p}}_e}\,. \tag{16}$$

It is seen that the complexity of the centralized estimator is dominated by (8), which requires about $8N^3 + 40N^2$flops. The computational saving by decentralization up to this point has been attained through the reduction of a $2N$-dimensional TDOA/FDOA measurement space to N 2-dimensional TDOA/FDOA measurement spaces. More significant is the reduction of exchange of raw data among sensors in the network, which now occurs only between the two paired sensors.

B. Suboptimal aggregation of decentralized estimates

Each of the decentralized estimate $\hat{\mathbf{p}}_e^j$ is now viewed as a measurement of an unknown quantity $\mathbf{p}_e$, in the presence of a random, independent, and unbiased additive measurement error of covariance P^j. The goal is to find an estimate of the form

$$\hat{\mathbf{p}}_e = \sum_{j=1}^{N} k_j \hat{\mathbf{p}}_e^j$$

that minimizes variance $E\{\|\mathbf{p}_e - \hat{\mathbf{p}}_e\|^2\}$. The solution is easily shown to be the combined decentralized estimates given by [4]

$$\hat{\mathbf{p}}_e \equiv P\left[\sum_{j=1}^{N}(P^j)^{-1}\hat{\mathbf{p}}_e^j\right], \quad P^{-1} \equiv \sum_{j=1}^{N}(P^j)^{-1}. \tag{17}$$

Though the estimate in (17) has been given the minimum variance interpretation, the above combined estimate is not equivalent to the optimal estimate from a centralized estimator in (6) because of the common quantity to be estimated. The coupling among the estimates can be observed from (8). However, an upper bound of the mean square error of the aggregated estimation can be explicitly calculated based only on the decentralized covariances as follows [15]

$$E\{\|\mathbf{p}_e - \hat{\mathbf{p}}_e\|^2\} \le \sum_{j=1}^{N} \kappa_j^* \ \text{trace}\ [P(P^j)^{-1}P] \tag{18}$$

where

$$\kappa_j^* = \frac{\sum_{l=1}^{N}\sqrt{\zeta_l^T P^l \zeta_l}}{\sqrt{\zeta_j^T P^j \zeta_j}}, \ j = 1,2,\cdots,N. \tag{19}$$

and vector $\zeta_l \neq 0$, $\forall l$. In particular, $\kappa_j^* = N$ can always be used, which yields the following (generally conservative) covariance bound

$$Cov\{\mathbf{p}_e - \hat{\mathbf{p}}_e\} \le NP, \tag{20}$$

though one may find the minimizing κ^* using semidefinite programming [15] to tighten the bound.

The aggregation process requires that each sensor pair sends its decentralized estimate $\hat{\mathbf{p}}_e^j = (\hat{x}_e^j, \hat{y}_e^j)$ and its 2×2 error covariance P^j to a common node, where a simple operation dictated by (17) is performed. If the aggregated estimation error falls within the tolerance set by a stopping criterion, the localization mission is complete. Otherwise, the aggregated estimate $\hat{\mathbf{p}}_e$ and covariance P are fed back to the sensors for use in (15) to continue into the next round of acquisition and estimation. Such a feedback of highly compressed data has been named federation in [4].

An immediate benefit of the decentralized sensing scheme together with the use of the above aggregation scheme is an enhanced sensor system ability to tolerate loss of vehicles. In case of the loss of sensor pair j, P^j is infinitely large and thus the contribution of the sensor pair is removed according to (17). Network tolerance also applies to data loss. If data

are lost from sensor pair j, pair j makes no contribution to the aggregated estimate; if data are lost on the way to sensor pair j, the next estimate from sensor pair j is discounted.

C. Velocity reachable sets

Suppose the stopping criterion is not met upon obtaining an emitter location estimate. Another round of sensing and estimation starts immediately, unless a pre-set mission time limit has been reached. This subsection describes the prelude to the third event in Fig.2. It is only necessary to consider a single vehicle at a time to determine what is the set of possible velocities reachable by the vehicle for a given set of time, speed, thrust constraints, and an initial velocity.

The vehicle dynamics is described as a point mass in level flight

$$\dot{u}_i = T_i \cos\psi_i, \dot{v}_i = T_i \sin\psi_i, \tag{21}$$

where ψ_i is the heading angle under the assumption of zero side-slip angle, and T_i is the thrust for which vector thrusting is assumed ($\psi_i \in [0, 2\pi]$).

To improve a new estimate of the emitter location by the same pair of sensors, it is necessary to allow the sensors sufficient time to change their velocities. On the other hand, to uphold the velocity dominance, sensor state update interval must be confined to a small value. Taking into all practical considerations in this application, the update interval is chosen in the range of a few seconds to a few tens of a second. With the addition of a time constraint, a reachable set from any initial velocity (u_i, v_i) at $\tau = 0$ is now fully defined

$$\mathscr{A}_i(\tau) = \{(u_i^+, v_i^+) | \sqrt{(u_i^+)^2 + (v_i^+)^2} \le S_{max}, T_i \le T_{max}, t \le \tau\}, \tag{22}$$

where τ, T_{max}, and S_{max} represent time, thrust magnitude, and speed upper bounds, respectively. Note that a lower speed limit is not imposed to retain the convexity of the velocity reachable set. There are several types of UAVs that can in fact hover [12], though a very low speed has never been encountered in our simulation study with thousands of replications.

The boundary of $\mathscr{A}_i(\tau)$ can be solved from a bang-bang optimal control problem. The switching time needed for thrusting from T_{max} to $T_i = 0$ for a fixed heading angle ψ_i is

$$\begin{aligned} t_{s,i} &= \frac{1}{T_{max}} \{ \sqrt{S_{max}^2 - (u_i^2 + v_i^2)[1 - \cos^2(\psi_i - \tan^{-1}\frac{v_i}{u_i})]} \\ &- \sqrt{(u_i^2 + v_i^2)} \cos(\psi_i - \tan^{-1}\frac{v_i}{u_i}) \}. \end{aligned} \tag{23}$$

Velocity (u_i^+, v_i^+) at final time τ is

$$u_i^+(\tau) = \begin{cases} u_i + t_{s,i} T_{max} \cos\psi_i, & t_{s,i} < \tau \\ u_i + \tau T_{max} \cos\psi_i, & t_{s,i} \ge \tau \end{cases} \tag{24}$$

$$v_i^+(\tau) = \begin{cases} v_i + t_{s,i} T_{max} \sin\psi_i, & t_{s,i} < \tau \\ v_i + \tau T_{max} \sin\psi_i, & t_{s,i} \ge \tau \end{cases} \tag{25}$$

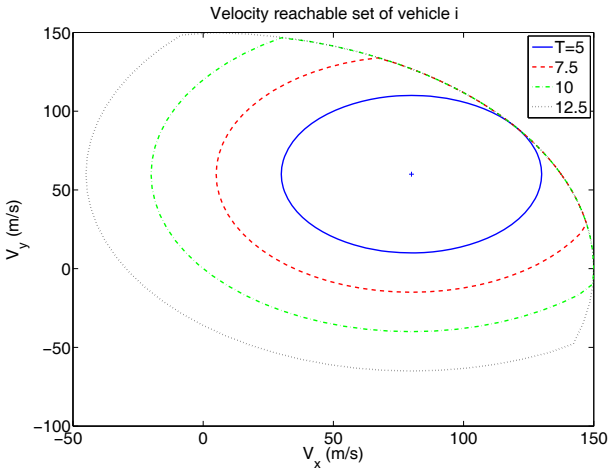

Fig. 3. Velocity reachable set for vehicle i at $\tau = 5$ sec., 7.5 sec., 10 sec., and 12.5 sec., respectively, from initial velocity $(80, 60)$ m/sec. at $\tau = 0$.

Fig.3 shows an example of nested reachable sets for $\tau = 5$ sec., 7.5 sec., 10 sec., and 12.5 sec., respectively, from an initial velocity at $(80, 60)$ m/sec., with $T_{max} = 10$ m/sec./sec. (thrust and acceleration are not distinguished for the point mass system), and $S_{max} = 150$ m/sec.

D. Decentralized sensor trajectory generation and vehicle maneuver

This subsection concerns the third event in Fig.2. Sensor trajectories are generated through a sequence of sensor state updates. A major benefit of decentralization, other than fault-tolerance, is the significant simplification in computing the projected sensor states in the process of creating trajectories for the vehicles to follow. The process now involves only the two velocities of an individual pair of sensors, thus simplifies (12) to

$$\min_{\substack{(u_{2j-1}^+, v_{2j-1}^+) \in \mathscr{A}_{2j-1}(\tau) \\ (u_{2j}^+, v_{2j}^+) \in \mathscr{A}_{2j}(\tau)}} V(\hat{\mathbf{p}}_e, (u_{2j-1}^+, v_{2j-1}^+), (u_{2j}^+, v_{2j}^+)) \tag{26}$$

More specifically, from (11), the objective function to be minimized for the jth sensor pair is

$$|[P^{-1}(\hat{\mathbf{p}}_e, \mathbf{z}) + G^T(\hat{\mathbf{p}}_e; \mathbf{z}_{2j-1}^+, \mathbf{z}_{2j}^+)(C^j)^{-1} G(\hat{\mathbf{p}}_e; \mathbf{z}_{2j-1}^+, \mathbf{z}_{2j}^+)]^{-1}|, \tag{27}$$

for which explicit expressions for the entries of $G(\hat{\mathbf{p}}_e; \mathbf{z}_{2j-1}^+, \mathbf{z}_{2j}^+)$ can be derived from (1), (2), and (9) [9]. Though (27) is generally not a function jointly convex in $\mathbf{z}_{2j-1}^+$, and $\mathbf{z}_{2j}^+$, it is a quadratic function of only 4 variables, and therefore the optimal point can be directly searched in the Cartesian product space containing $\mathscr{A}_{2j-1}(\tau)$ and $\mathscr{A}_{2j}(\tau)$, whereas the original centralized optimization of (13) involves $8N$ variables and a much more complex objective function.

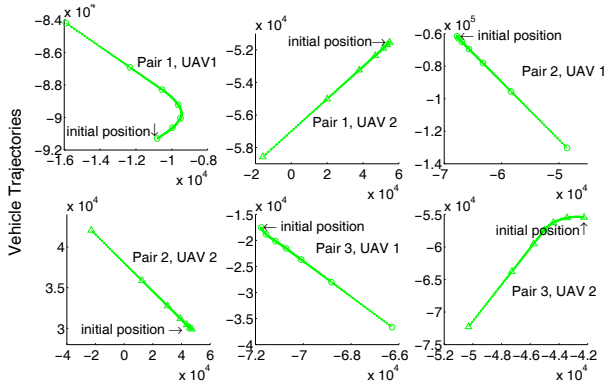

Fig. 4. Sample trajectories of a 6 UAV location sensor network for which the vehicles are maneuvered from their initial velocities to their optimized velocities in six consecutive updates of $\tau = 10$ sec. each. The axes are x and y positions in meters.

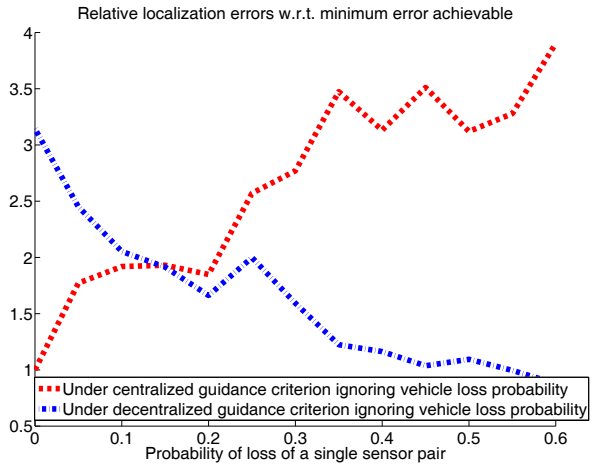

Fig. 5. Ratios of localization errors under a centralized guidance criterion (red) and a decentralized (blue) guidance criterion, both of which ignore the information on the probability of loss of vehicles, to that under a centralized guidance criterion weighed by vehicle loss probabilities

The last step is to determine the thrusts needed to reach $\mathbf{z}^+$. Let $t' = \max_i t'_i \leq \tau$, where t'_i is the minimum time for sensor i to reach its final velocity (u_i^+, v_i^+) from its initial velocity (u_i, v_i). Assume optimally projected velocities of some of vehicles lie in the interior of their respective velocity reachable sets. (24) or (25) can now be used to adjust T_{max} to

$$T_{max,i} = (t_{s,i}/t')T_{max} \leq T_{max}$$

for those projected velocities that lie on the boundaries of their respective reachable sets, such that all vehicles arrive at their destinations

$$(u_i^+(t'), v_i^+(t')) = (u_i + t'T_{max,i}\cos\psi_i, v_i + t'T_{max,i}\sin\psi_i)$$

at t'. If all optimally projected velocities are on the boundaries of the corresponding velocity reachable sets with $t_{s,i} < \tau$ $\forall i$, $t' = \max_i t_{s,i}$, and no adjustment on T_{max} is needed; otherwise, $t' = \tau$. In fact $t' = \tau$ can always be used with downward scaling of T_{max} to $T_{max,i}$ for some of the i's to control all vehicles to arrive at there destinations in exactly τ seconds without switching off thrust.

E. Performance analysis through an example of a 6-sensor network

Fig.4 shows a set of sample trajectories of a 6-sensor network for which the vehicles are maneuvered from their initial velocities to their optimized velocities in six consecutive updates of $\tau = 10$ seconds each. Using (13), localization accuracy is improved from initial area of a 50% concentration ellipse ($Pr[\mathbf{p} \in R_{\ln 4}] = 0.5$) at 350 m^2 to less 10 m^2 after 60 seconds and 6 rounds of target signal acquisition.

In this study, signal-to-noise ratio is set at $8 \sim 10$ dB, maximum vehicle speed is set at 150 m/s, maximum acceleration is set at 10 m/s^2, and time interval between state update is fixed at 10 seconds. Initial guess of emitter location is $2.5 \sim 5$ km away from the true location. All sensing carrying vehicles are $50 \sim 100$ km away from the emitter location. The initial velocities of the vehicles are set randomly at $100 \sim 150$ m/s with a random direction, and the probability of loss of a sensor pair within an update interval is varied from $0\% \sim 60\%$.

Comparison of localization errors between centralized sensing (red), and decentralized sensing (blue) is made through their relative errors, which are the ratios of the calculated areas of the 50% concentration ellipses in each case to that of the centralized sensing using the vehicle loss probability-weighted guidance criterion (13) and a centralized location estimator, respectively. Fig.5 shows the calculated areas of the 50% concentration ellipses of 100 independent replications for a discrete set of values of probability of loss of a pair. As the probability of loss of a sensor pair increases, the result of aggregation moves toward optimality. It is seen that decentralized sensing (blue) gains better accuracy than the centralized sensing (red) as the probability of loss of a sensor pair increases beyond 0.15 when the loss probability is disregarded in the localization process. Fig.6 shows a snap shot of the 50% concentration ellipses at a given probability of loss of vehicles of the three localization schemes.

IV. Discussion and Conclusions

The previous section has discussed the most salient advantages of decentralized sensing of time/frequency-based airborne location sensors: reduction of computation and communication complexity and tolerance to vehicle loss.

The paper concludes with a more general qualitative argument on the benefit of decentralization, especially with regard to tolerance to loss of sensors. As the probability of loss of a single pair of sensors p increases, the terms corresponding to a single remaining pair of sensors in

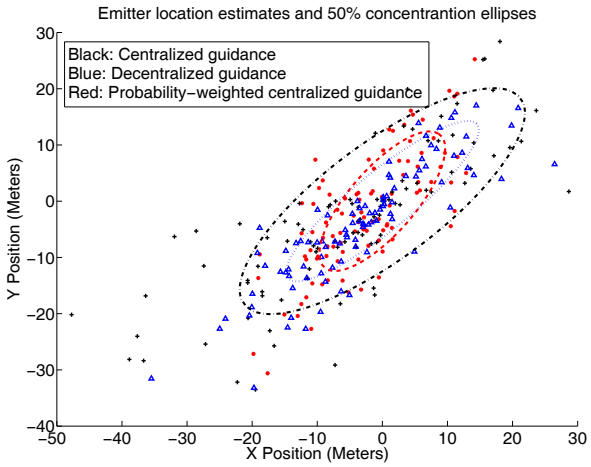

Fig. 6. Emitter location estimates and concentration ellipses of the 100 replications for decentralized sensing (blue), centralized sensing (black), and probability-weighted centralized sensing with the probability of loss of a sensor pair set at 0.35

the weighted criterion (13) become increasingly dominant, approaching the decentralized criterion (12) for projected sensor state calculations. At the same time the aggregation in (17) for the decentralized sensing reduces to that of a single pair network, so is the centralized sensing in (6)–(8), due to loss of useful measurements from the remaining sensors pairs in (3).

V. Acknowledgment

This work was supported in part by the US Air Force Office of Scientific Research under Grants FA9550-06-0456 and FA9550-06-1-0249.

VI. References

[1] R.W. Beard, T.W. McLain, D.B. Nelson, D. Kingston, and D. Johanson, Decentralized cooperative aerial surveillance using fixed-wing miniature UAVs, *Proceedings of the IEEE*, vol.94, pp.1306-1324, 2006.

[2] Bertsekas, D.P., *Dynamic Programming and Optimal Control*, Volume 1 & Volume 2, Athena Scientific, 1995.

[3] S.P. Boyd, and L. Vandenberghe, *Convex Optimization*, Cambridge University Press, 2004.

[4] N.A. Carlson, Federated square root filter for decentralized parallel processes, IEEE Trans. Aerospace and Electronic Systems, Vol.26, pp.517-525, 1990.

[5] T.M. Cover, and J.A. Thomas, *Elements of Information Theory*, John Wiley & Sons, 1991.

[6] H. Durrant-Whyte, and T. Bailey, Simultaneous Localisation and Mapping (SLAM): Part I The Essential Algorithms. *Robotics and Automation Magazine*, vol.13, pp.99110, 2006.

[7] J.L. Farrell, J.H. Mims, and A. Sorrell, Effects of navigation errors in maneuvering SAR, *IEEE Transactions on Aerospace and Electronic Systems,* vol.9, pp.758-776, 1973.

[8] M.L. Fowler, and M. Chen, Evaluating Fisher information from data for task-driven data compression, *Proceedings of Conference on Information Sciences and Systems*, 2005.

[9] K. Huang, N.E. Wu, and M.L. Fowler, Optimal Guidance of Unmanned Vehicles for Emitter Location, *Proc. 17th IFAC World Congress*, 2008.

[10] S.M. Kay, *Fundamentals of Statistical Signal Processing: Estimation Theory*, Prentice Hall, 1988.

[11] R.A. Poisel, *Electronic Warfare Target Location Methods*, Artech House, 2005.

[12] T. Samad, J.S. Bay, and D. Godbole, Network-centric systems for military operations in urban terrain: the role of UAVs, *Proceedings of the IEEE*, vol.95, pp.92-107, 2007.

[13] D.J. Torrieri, Statistical theory of passive location systems, *IEEE Transactions on Aerospace and Electronic Systems,* vol.20, pp.183-198, 1983.

[14] S. Stein, Differential delay/Doppler ML estimation with unknown signals, *IEEE Transactions on Signal Processing*, vol.41, pp.2717-2719, 1993.

[15] N.E. Wu, and M.L. Fowler, An Error bound for sensor fusion with application to Doppler frequency based emitter location. *IEEE Transactions on Automatic Control*, vol.51, pp.631-635, 2006.

[16] N.E. Wu, and M.L. Fowler, Aperture error mitigation via local-state estimation for frequency-based emitter location, *IEEE Transactions on Aerospace and Electronics*, vol.39, pp.414-428, 2003.

[17] N. E. Wu, Y. Guo, K. Huang, M. C. Ruschmann, and M. L. Fowler, Fault-tolerant tasking and guidance of an airborne location sensor network, Special Issue on Fault Detection, Diagnosis, and Fault-Tolerant Control, *International Journal of Computation, Automation, and Systems*, 2008.

[18] N.E. Wu, Y. Zhang, K. Zhou, Detection, estimation, and accommodation of loss of control effectiveness, *International Journal Of Adaptive Control And Signal Processing*, vol.14, pp.775-795, 2000.